ELSEVIER

Coordination Chemistry Reviews
190–192 (1999) 1169–1184

COORDINATION CHEMISTRY REVIEWS

www.elsevier.com/locate/ccr

Valence transition with charge ordering in a conductive MMX-chain complex

Hiroshi Kitagawa *, Tadaoki Mitani

Department of Physical Materials Science, School of Materials Science, Japan Advanced Institute of Science and Technology, Asahidai 1-1, Tatsunokuchi, Ishikawa 923-1292, Japan

Received in revised form 17 May 1999

Contents

Abstract

The charge ordering states with lattice distortions in a halogen-bridged binuclear-metal mixed-valence complex (called an MMX-chain), $Pt_2(dta)_4I$ ($dta = CH_3CS_2^-$), have been investigated by transport, magnetic, and optical measurements. This complex exhibits metallic conduction above room temperature and represents the first example of a metallic

* Corresponding author. Tel.: +81-761-51-1532; fax: +81-761-51-1149.
E-mail address: hiroshi@jaist.ac.jp (H. Kitagawa)

0010-8545/99/$ - see front matter © 1999 Elsevier Science S.A. All rights reserved.
PII: S0010-8545(99)00174-5

halogen-bridged 1-D transition-metal complex. Below 300 K it shows semiconducting behavior, which is considered to be of the Mott-Hubbard type due to electron correlation. The metal–semiconductor transition at 300 K ($= T_{M-I}$) is derived from a valence transition of Pt from an averaged-valence state of $+2.5$ to a trapped-valence state of $+2$ and $+3$. The charge ordering modes are considered to be $-I-Pt^{2+}-Pt^{3+}-I-Pt^{2+}-Pt^{3+}-I-Pt^{2+}-Pt^{3+}-I-Pt^{2+}-Pt^{3+}-I-$ for the semiconducting phase below T_{M-I} and $-I-Pt^{2.5+}-Pt^{2.5+}-I-Pt^{2.5+}-Pt^{2.5+}-I-Pt^{2.5+}-Pt^{2.5+}-I-Pt^{2.5+}-Pt^{2.5+}-I-$ for the metallic phase above T_{M-I}. The low-temperature electronic structure at 80 K is considered to be an alternate charge ordering state of $-I-Pt^{2+}-Pt^{3+}-I-Pt^{3+}-Pt^{2+}-I-Pt^{2+}-Pt^{3+}-I-Pt^{3+}-Pt^{2+}-I-$. The vibronic state in the intermediate phase is also discussed. © 1999 Elsevier Science S.A. All rights reserved.

Keywords: Mixed valence; Molecular conductor; MX-chain; Charge ordering; Mott transition; Binuclear metal complex

1. Introduction

Halogen-bridged one-dimensional (1-D) transition-metal complexes, the so called MX-chain compounds, provide a unique opportunity to investigate 1-D electron–electron or electron-lattice correlated systems [1–3]. One of the most important features of the MX-chain materials is that their electronic structures can be controlled by varying their constituents, e.g. the transition-metal ions, the bridging halogen ions, the terminal ligands, the counter ions, and possibilities for intrachain or interchain hydrogen bonds. In fact, the optical energy gap can be changed widely from 0.8 to 3.3 eV in MX-chain materials [4]. The photo-excited state of the MX-chain is very dynamic, due to strong electron-lattice interaction, especially for M = Pd and M = Pt, that investigations have been focused on their optical properties; examples including intense and dichroic intervalence charge-transfer (IVCT) absorption [5–7], progressive resonance Raman scattering [8–10], luminescence with large Stokes shift [11,12], midgap absorptions [13–17] originating from solitons or polarons, and large third-order nonlinear optical properties [18]. On the other hand, the control of energy gap in the lower-energy region near zero or equal to zero has not been attained. In such a system, a dynamical valence fluctuation of the metal ions is expected in the ground state.

As shown in Fig. 1, if we imagine a hypothetical metallic chain with no Peierls distortion, the half-filled conduction band is made up primarily of an antibonding combination of transition-metal dz^2-orbitals and bridging halogen pz-orbitals. But in practice, MX-chains with M = Ni are Mott-Hubbard or charge-transfer-type insulators (which is called the spin-density wave (SDW) state by some physicists) due to strong electron correlation, that is, on-site Coulomb repulsion (U) [19–21]. On the other hand, MX-chains with M = Pd, Pt are mixed-valence-type insulators (which is called the charge-density wave (CDW) state) in which the charge ordering of $\cdots X-M^{4+}-X\cdots M^{2+}\cdots$ occurs and opens a gap at the Fermi energy due to the strong electron-lattice interaction, i.e. negative-U effect [22–24]. Up to now, no metallic transport in these systems has been observed.

In this paper, we focus on a mixed-valence MMX-chain system $Pt_2(dta)_4I$ which has 1-D $-I-Pt_2(dta)_4-I-Pt_2(dta)_4-I-$ ($dta = CH_3CS_2^-$, dithioacetate) chains, as shown in Fig. 2. The formal oxidation state of the Pt ions is $+2.5$. This material has a neutral-chain structure and a helical arrangement of four dta-ligand planes around the central Pt–Pt axis. This was first synthesized and its basic properties studied by Bellitto et al. [25] in 1982. Subsequently the Ni analog was characterized by the same authors in 1985 [26]. According to our recent work [27–30], the Pt salt was found to exhibit metallic conduction around room temperature (r.t.), which is the first observation of a metallic halogen-bridged 1-D transition-metal complex. While the MX-chain is a mononuclear unit-assembled system, the MMX-chain is a binuclear unit-assembled system containing metal–metal bonds, so that internal degrees of freedom in dimer units can be increased. Such the 1-D mixed-valence polynuclear unit-assembled conductor may be expected to be a spin-charge-lattice coupled system with a dynamical electronic state.

A wide variety of possible electronic structures can be expected in the MMX-chain. Some of the possible 1-D charge ordering states for the MMX-chain are shown below, and also for the MX-chain. It is noted that the valence numbers show formal oxidation states. Since the charge transfer occurs between the metals through bridging X, the numbers should be expressed in the net charge. For example, $(2+\delta)+$ and $(4-\delta)+$ instead of $2+$ and $4+$ for the MX-chain and

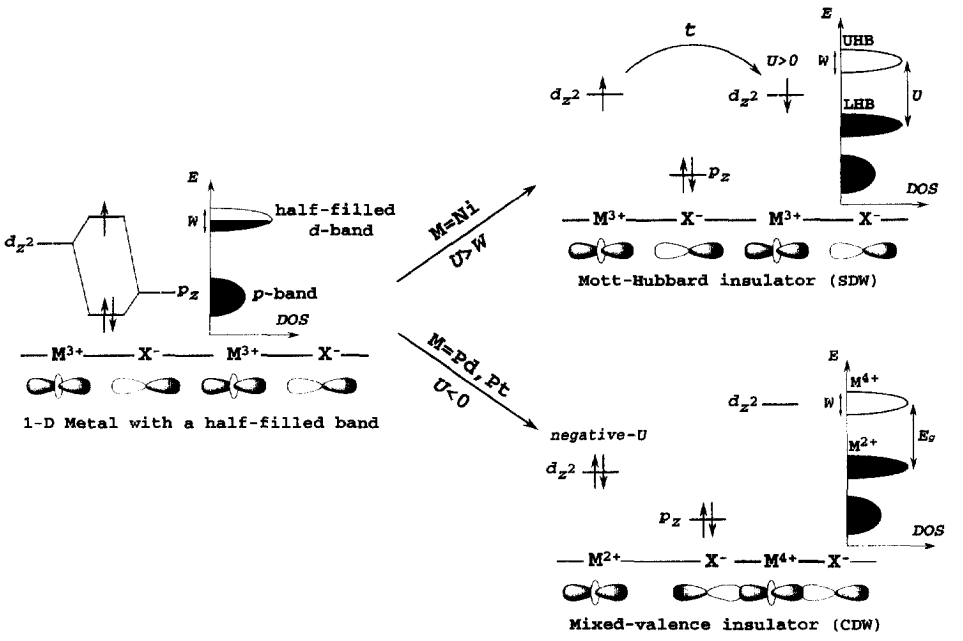

Fig. 1. Schematic electronic structures for a 1-D metal with a half-filled d-band in the MX-chain, a Mott-Hubbard insulator (SDW), and a mixed-valence insulator (CDW). UHB, LHB, and DOS abbreviate upper Hubbard band, lower Hubbard band, and density of states, respectively.

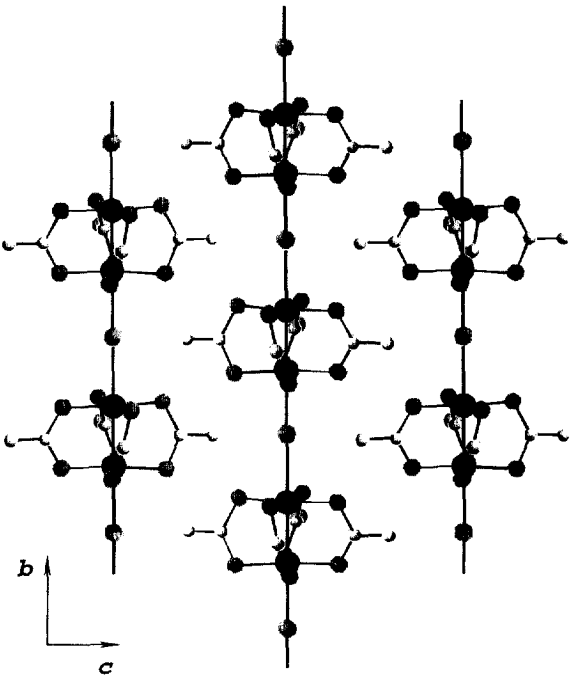

Fig. 2. Crystal structure of $Pt_2(dta)_4I$ in the projection of the *bc* plane [26].

$(2+\delta')+$ and $(3-\delta')+$ instead of $2+$ and $3+$ for the MMX-chain, respectively $(0 \leq \delta \leq 1,\ 0 \leq \delta' \leq 0.5)$. Representations of possible charge ordering modes in:

MX-chains

(1) $-X-M^{3+}-X-M^{3+}-X-M^{3+}-X-M^{3+}-X-M^{3+}-X-M^{3+}-X-$

(2) $-X-M^{2+}-X-M^{4+}-X-M^{2+}-X-M^{4+}-X-M^{2+}-X-M^{4+}-X-$

MMX-chains

(1) $-X-M^{2.5+}-M^{2.5+}-X-M^{2.5+}-M^{2.5+}-X-M^{2.5+}-M^{2.5+}-X-M^{2.5+}-M^{2.5+}-X-$

(2) $-X-M^{2+}-M^{2+}-X-M^{3+}-M^{3+}-X-M^{2+}-M^{2+}-X-M^{3+}-M^{3+}-X-$

(3) $-X-M^{2+}-M^{3+}-X-M^{2+}-M^{3+}-X-M^{2+}-M^{3+}-X-M^{2+}-M^{3+}-X-$

(4) $-X-M^{2+}-M^{3+}-X-M^{3+}-M^{2+}-X-M^{2+}-M^{3+}-X-M^{3+}-M^{2+}-X-$

Considering the MMX-chains, the modes (1) and (2) have uniform charge distribution within the binuclear units, while modes (3) and (4) have charge-polarization. In the case of (2) and (3), the bridging halogens are expected to be deviated from the midpoints of two $[Pt_2(dta)_4]$ dimers due to the electron-lattice interaction, analogous to that observed in the MX-chain with M = Pt and X = I [31], while those of (1) and (4) situated at the midpoints. The charge ordering mode (1) is an averaged-valence state. Each binuclear-metal unit possess an unpaired electron (a

spin). In this case, the 1-D half-filled conduction band can be presumed to be composed primarily of an antibonding combination of antibonding $d\sigma^*$-orbitals of M(dz^2)–M(dz^2) and X(pz)-orbitals. Two possible electronic states are usually expected for mode (1); a Mott-Hubbard insulator ($U > W$ ca. $4t$ in a 1-D electronic system; W is the bandwidth and t is the transfer integral between metals) and a 1-D metal ($W > U$). The mode (2) is a mixed-valence insulating (CDW) state where cell doubling occurs. In mode (3) where there exists an unpaired electron (a spin) at the Pt^{3+} site per one dimer unit, no cell doubling occurs and therefore a Mott-Hubbard-type insulator or a 1-D metal is expected. The possibility of mode (4) is of much interest because of its analogy to a spin-Peierls state which has not been observed for MX-chain. In this case the binuclear units, having one spin per unit, are dimerized and this results in an alternate charge polarization. This state originates from spin-phonon interactions and nearest-neighbor inter-dimer Coulomb repulsion (V) [32,33].

From the interests mentioned so far, the physical properties in $Pt_2(dta)_4I$ were investigated by X-ray photoelectron spectroscopy (XPS), electrical conductivity, thermoelectric power, SQUID magnetometry, polarized Raman spectroscopy, IR spectroscopy, and ^{129}I Mössbauer spectroscopy measurements.

2. Experimental

The title complex was prepared by the method previously reported [25].

The X-ray photoelectron spectroscopy (XPS) measurements were carried out on a VG ESCA MKII electron spectrometer at the Institute for Molecular Science with a Mg–Kα X-ray source (1253.6 eV).

The dc electrical-conductivity measurements were performed along the b axis (//chain) by a conventional four-probe method.

The thermoelectric power measurement was made by a dynamical differential method.

Polarized Raman spectra of single crystals were recorded with a Jasco NR-1800 subtractive-dispersion triple (filter single) polychromator using a microscope. A Spectra-Physics model 2017 Ar^+ laser provided the exciting line (514.5 nm). The Z(YY)$\bar{Z}$ and Z(XX)$\bar{Z}$ components of the scattered radiation were used, where X//c^*, Y//b^*, Z//$a^* - c^*$ (ca. a), and the 1-D chain //b^* ($= b$).

For IR absorption spectra, powdered samples ground down from single crystals were diluted with KBr and then the mixtures were processed into pellets under pressure and vacuous condition.

The magnetic susceptibility measurement of a polycrystalline sample was performed in the temperature range of 4–400 K on a Quantum Design MPMS-5 SQUID magnetometer.

Mössbauer spectroscopic measurements of the 27.7 keV transition in ^{129}I were carried out with both source and absorber cooled down to 80 K by using a constant-acceleration spectrometer with a NaI(Tl) scintillation counter.

3. Results and discussions

3.1. XPS spectroscopy

In order to investigate the mixed-valence state of $Pt_2(dta)_4I$, XPS measurements were carried out at r.t. Fig. 3 shows the XPS spectra of Pt 4f region for $Pt_2(dta)_4I$ and the Pt^{2+} control complex, $Pt(H_2DAG)_2Cl_2$ (H_2DAG = diaminoglyoxime). As can be seen in Fig. 3(b), the doublet is much broader having FWHMs of 1.92 and 2.75 eV for $4f_{7/2}$ and $4f_{5/2}$, respectively, compared with the spectrum (Fig. 3(c)) of

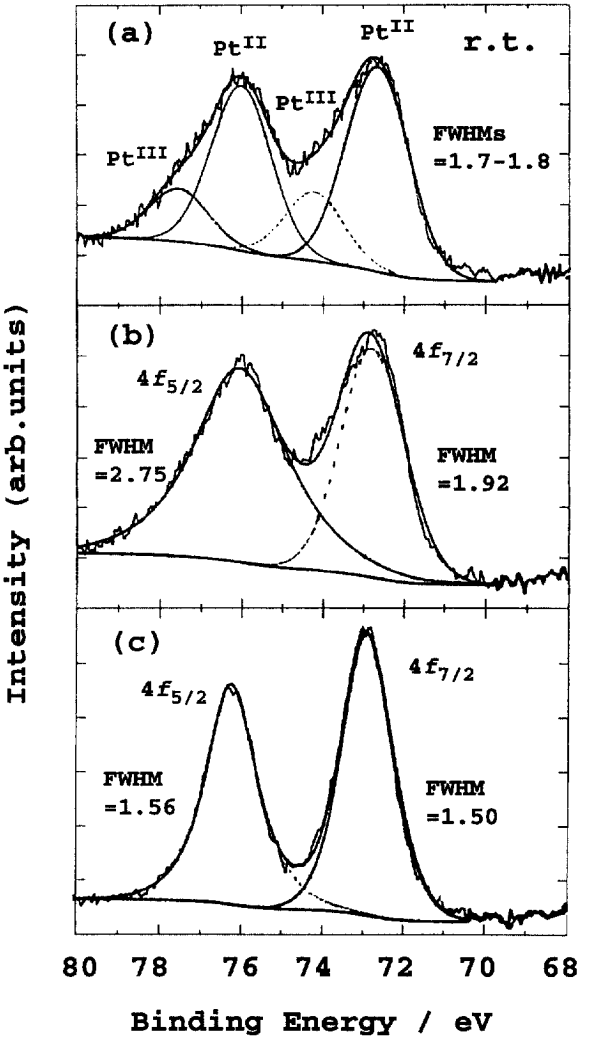

Fig. 3. XPS spectra of Pt 4f region at r.t, (a) a fit with two doublets for the observed spectrum of $Pt_2(dta)_4I$, (b) a fit with one doublet for the same spectrum of (a), (c) $Pt(H_2DAG)Cl_2$.

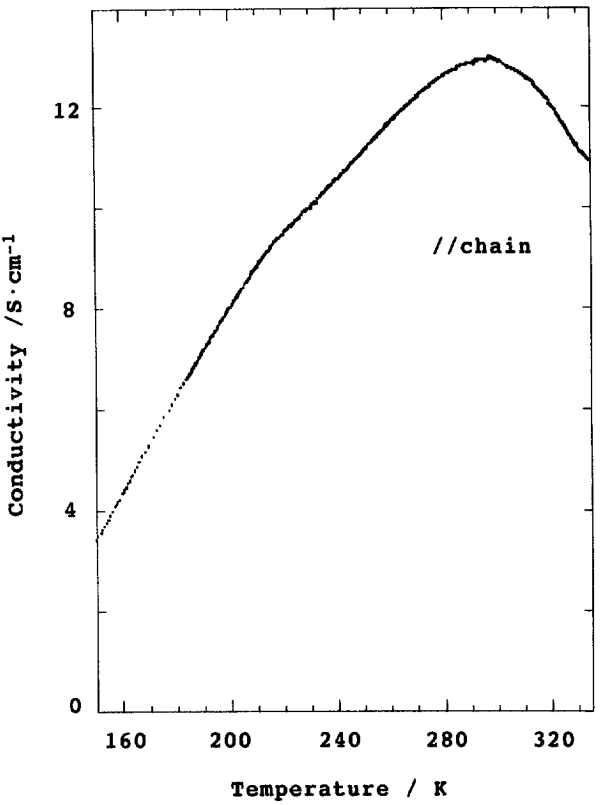

Fig. 4. Temperature dependence of the electrical conductivity of $Pt_2(dta)_4I$ parallel to the chain axis *b*.

the Pt^{2+} control complex (1.50 and 1.56 eV, respectively). The observed spectrum at r.t. was reasonably resolved into signals for Pt^{2+} and Pt^{3+} by using peak-decomposition software. The binding energies of the doublet decomposed on the higher energy side are typical ones for Pt^{3+} compounds. The intensity of the Pt^{3+} signal is smaller than that of Pt^{2+}, probably due to some decomposition (Pt^{3+} is partially reduced to Pt^{2} by the X-ray beam despite careful measurements). It is noted that the mixed-valence complex $K_2Pt(CN)_4 \cdot Br_{0.3} \cdot 3.2H_2O$, which is a metallic molecule-based conductor, shows XPS spectra composed of two signals of Pt^{2+} and Pt^{4+} [34], because of a rapid time scale (ca. 10^{-17} s) of the XPS experiment.

3.2. Transport properties

Fig. 4 shows the temperature dependence of the electrical conductivity parallel to the chain axis (*b*) for the single crystal of $Pt_2(dta)_4I$. The r.t. conductivity is 13 S cm^{-1}, which is about nine orders of magnitude higher than the typical value of a MX-chain complex. This complex undergoes a metal–semiconductor transition at 300 K ($= T_{M\text{-}I}$). Above $T_{M\text{-}I}$ it exhibits metallic conduction. A slight knee is

observed around 230 K, which is considered to be a transition from a low-temperature ordered phase to an intermediate partially disordered one (mentioned in Section 3.7).

A typical result of the thermoelectric power S as the function of the temperature in $Pt_2(dta)_4I$ is shown in Fig. 5. The metal–semiconductor transition was also confirmed by the temperature dependence of S. When $T < 300$ K, the thermoelectric power increases significantly from negative values to positive ones with cooling. The divergent change below 300 K is indicative of the opening of a gap at the Fermi energy.

3.3. Magnetic properties

In order to clarify the origin of the metal–semiconductor transition observed at 300 K, the temperature dependence of magnetic susceptibility was measured and is displayed in Fig. 6. The data are corrected for the ligand and metal core diamag-

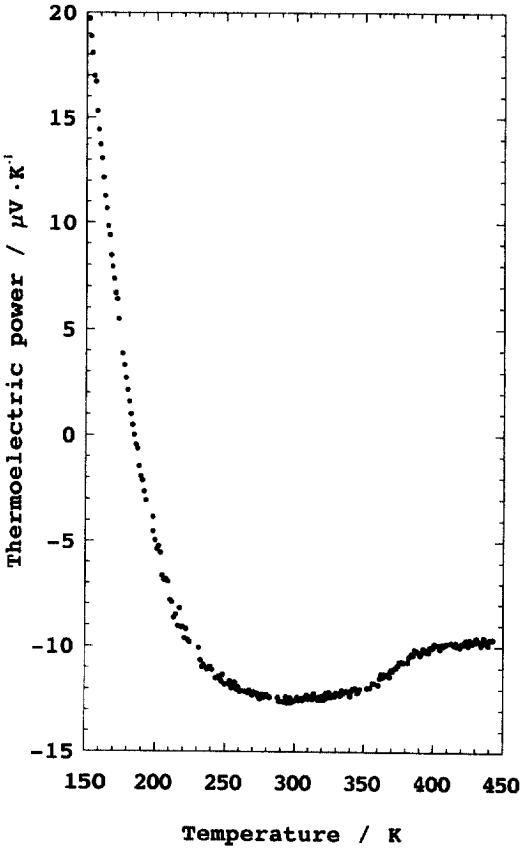

Fig. 5. Temperature dependence of the thermoelectric power of $Pt_2(dta)_4I$ parallel to the chain axis b.

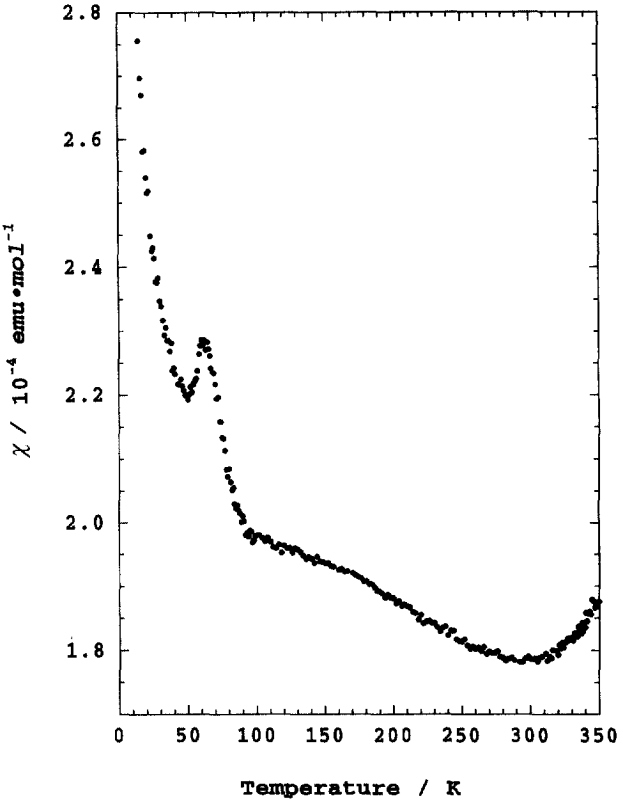

Fig. 6. Temperature dependence of the magnetic susceptibility of $Pt_2(dta)_4I$.

netic contributions which are estimated at -4.04×10^{-4} (emu mol^{-1}), the sum of the measured value of $Pt_2(dta)_4$ and half the reference value of I_2. In the metallic region of $300 < T < 350$ K, the susceptibility decreases with temperature, which has been often observed in 1-D molecular conductors. Typically, the temperature dependence of the susceptibility in 1-D molecule-based conductors deviates considerably from Pauli temperature-independent paramagnetism [35]. Below $T_{M\text{-}I}$, the magnetic susceptibility increases slightly with a slight convexity in the $\chi_s - T$ curve upon cooling down to 90 K. If a transition relates to a Peierls (CDW) instability, the spin susceptibility should be activated below the transition because of the freezing of both charge and spin degrees of freedom. The opposite behavior was observed. Since only the charge degree of freedom is lost at $T_{M\text{-}I}$ and the spin one survives, the semiconducting state can be considered to be a $4k_F$ CDW, that is a Mott-Hubbard insulator in a half-filled band with magnetic disorder. In the case of a Mott transition, the translational symmetry of the binuclear unit is maintained, so either mode (1) or (3) can be the semiconducting state just below $T_{M\text{-}I}$. Below 90 K, the susceptibility increases rather rapidly down to 20 K and then increases rapidly to 4.2 K due to a small amount of paramagnetic impurities. There seems to be some evidence of a transition at 90 K.

3.4. Polarized Raman spectroscopy

Raman spectroscopy has been used widely to study the vibrational and structural properties of MX-chain or MMX-chain compounds [36]. Raman modes are very sensitive to the symmetry of the metal-complex unit and its translational geometry. The Pt–Pt distances of the $[Pt_2(dta)_4]$ dimer units in mode (1), (3) or (4), are uniform, so that the Pt–Pt stretching mode, ν(Pt–Pt), would be a singlet. In case of mode (2), on the other hand, the Pt–Pt distances of the dimer units are different from one another, so that the ν(Pt–Pt) mode would be a doublet. In addition, if the iodine ions were centrally placed between the $[Pt_2(dta)_4]$ dimer units like mode (1) or (4), the symmetric Pt–I stretching mode, ν(Pt–I), would be Raman-inactive. The ν(Pt–I) mode would be Raman-active in case of mode (2) or (3). Accordingly, it seemed important to investigate the Raman spectra of this mixed-valence complex.

Fig. 7 shows the Raman spectra of Pt^{3+}–Pt^{3+} complexes $Pt_2(dta)_4X_2$ (X = Cl, Br, I) at r.t. Since the ν(Pt–X) mode is expected to shift to the lower wavenumber side in order of X = Cl > Br > I, the peaks of 185, 147, and 115 cm^{-1}, are respectively assigned to the ν(Pt–Cl), ν(Pt–Br), and ν(Pt–I) modes. The peaks

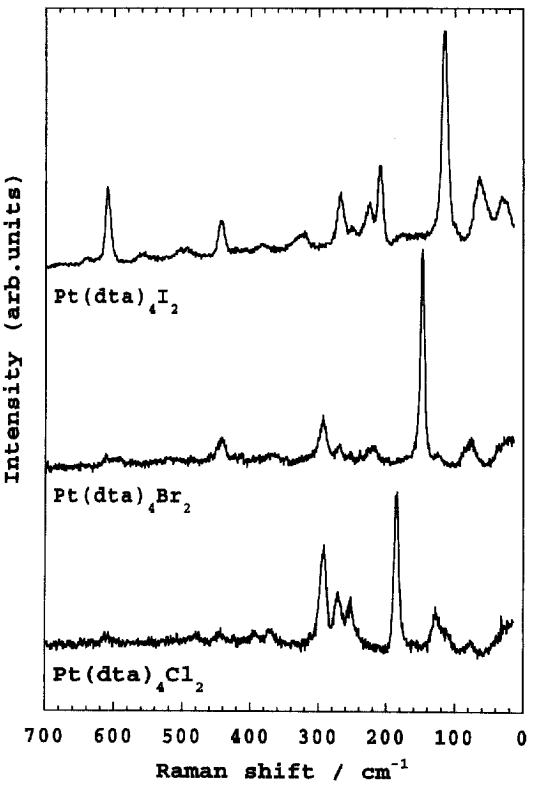

Fig. 7. Raman spectra of $Pt_2(dta)_4X_2$ (X = Cl, Br, I) at r.t.

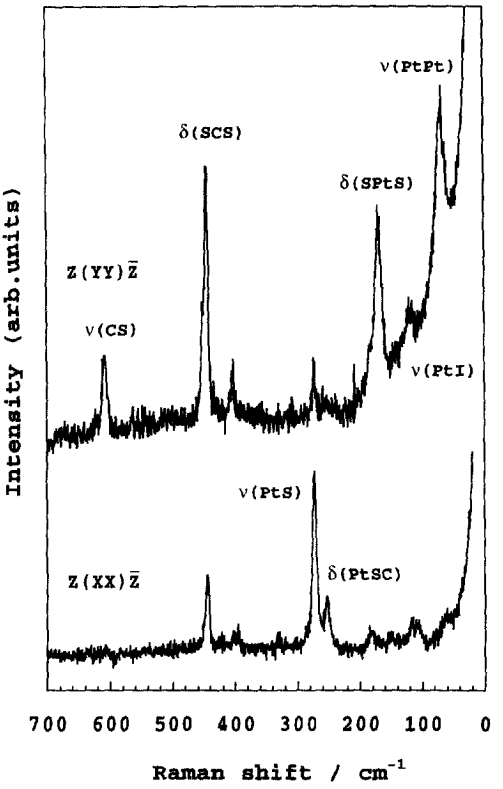

Fig. 8. Raman spectra of $Pt_2(dta)_4I$ at r.t. for the polarizations of $Z(YY)\bar{Z}$ and $Z(XX)\bar{Z}$.

observed around 70 cm^{-1} are unchanged in energy from X = Cl, X = Br, to X = I. A weak peak was also observed at 70 cm^{-1} for $Pt_2(dta)_4$. It is thereby reasonably assigned to ν(Pt–Pt). Fig. 8 shows the Raman spectra of $Pt_2(dta)_4I$ at r.t. (estimated just above T_{M-I}) for the polarizations of $Z(YY)\bar{Z}$ and $Z(XX)\bar{Z}$, in which the assignments are given. A very weak ν(Pt–I) mode at 119 cm^{-1} and no overtones were observed for the polarization of $Z(YY)\bar{Z}$ in $Pt_2(dta)_4I$. From these results, an important conclusion is drawn, i.e. that iodine ions can be centrally bridging between the $Pt_2(dta)_4$ units, otherwise the ν(Pt–I) mode would be strongly Raman-active. This is in good agreement with the results of the X-ray single-crystal analysis [25,37–39]. The Pt–Pt stretching mode is a singlet, and therefore the chain structure of the metallic state can be interpreted in terms of either model of mode (1) or mode (4) from the Raman study. The ν(Pt–Pt) mode is strongly y-polarized, which reflects a 1-D electron-lattice coupled system. It is noted that we have also studied another MMX-chain system, $A_4[Pt_2(pop)_4I]\cdot nH_2O$ (A = Li, Na, K, Rb, Cs, NH_4; pop = $H_2P_2O_5^{2-}$); The complexes with A = Cs and Rb show a doublet ν(Pt–Pt) mode and its overtones, while the others show a singlet ν(Pt–Pt) mode and no overtones. This may indicate that the former complexes have the charge ordering

mode (2). $K_4[Pt_2(pop)_4X]\cdot nH_2O$ (X = Cl, Br) complexes were also reasoned to have this ordering mode [40].

3.5. IR spectroscopy

Detailed information on the electronic structure can be also obtained from IR study. The IR modes of the ligand are very sensitive and provide a useful probe of the oxidation state of the metal. Therefore, we focused on the IR absorption spectra of C=S stretching mode in dta ligands of $Pt_2(dta)_4I$ in the temperature range from 11 to 475 K. As shown in Fig. 9, the C=S stretching mode at 1180 cm^{-1} was split into two bands below T_{M-I}. The IR mode of the CS_2 stretching vibration is considered to be quite sensitive and reflects the charge distribution of the intermetallic Pt–Pt bond in the $[Pt_2(dta)_4]$ dimer unit. The single peak observed above T_{M-I} strongly suggests that the electronic state has a uniform charge distribution,

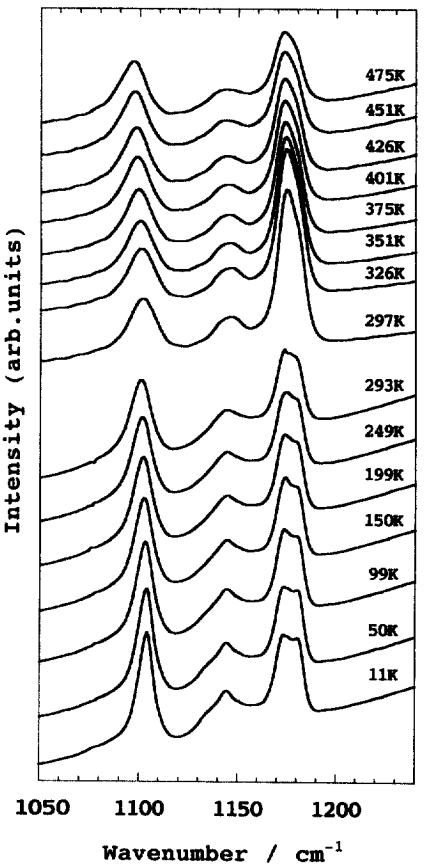

Fig. 9. Temperature dependence of the IR absorption spectra of the C=S stretching mode in the dta ligands of $Pt_2(dta)_4I$.

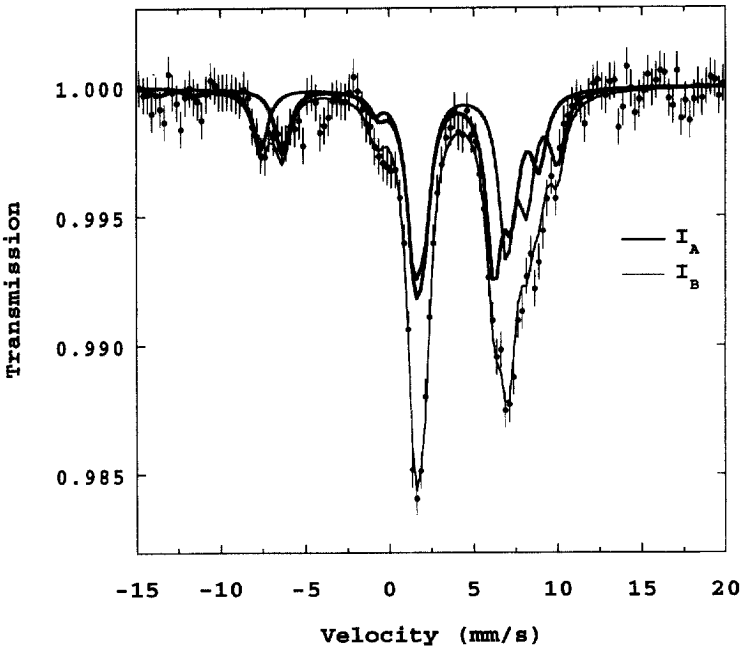

Fig. 10. ^{129}I Mössbauer spectra of $Pt_2(dta)_4I$ at 80 K.

that is mode (1). On the other hand, the two peaks observed below $T_{M\,I}$ show a trapped-valence state of Pt^{2+} and Pt^{3+}. This is evidence of a valence transition from an averaged-valence state to a trapped-valence state at T_{M-I}. So one of the modes (2)–(4) can be responsible for the semiconducting trapped-valence state. As discussed in Section 3.3, the semiconducting state is a Mott-Hubbard insulator. Accordingly, mode (3) is more favorable for the semiconducting state. Judging from Raman and IR studies, the metallic state has the averaged-valence mode (1).

3.6. *^{129}I Mössbauer spectroscopy*

In order to investigate the low-temperature charge ordering mode, a ^{129}I Mössbauer spectroscopic study was carried out. Comparatively, modes (2) and (3) have only one chemically distinct bridging iodine, while mode (4) has two including both Pt^{2+}–I–Pt^{2+} and Pt^{3+}–I–Pt^{3+} bridges. Unfortunately, experimental conditions of the 27.7 keV ^{129}I γ-ray resonance are limited to low temperatures, below 80 K, due to a poor recoil-free fraction. The observed ^{129}I Mössbauer spectra at 80 K are shown in Fig. 10. A best fit is obtained with two octuplets, which signifies the existence of two different iodine sites (I_A and I_B) in the MMX-chain and favors mode (4):

$$-Pt^{2+}-Pt^{3+}-I_A-Pt^{3+}-Pt^{2+}-I_B-Pt^{2+}-Pt^{3+}-I_A-Pt^{3+}-Pt^{2+}-I_B-Pt^{2+}-Pt^{3+}-$$

According to our preliminary measurement for $Ni_2(dta)_4I$, only one component of iodine was observed at 16 K, which implies a Mott-Hubbard insulating state of mode (1). From the present Mössbauer spectroscopic study, it can be concluded that the charge ordering mode (4) should be responsible for the semiconducting phase below 80 K. It should be noted that S.A. Borshch et al. have performed several kinds of calculations for a infinite chain and a four-nuclear cluster X_1–Pt_1–Pt_2–X_2–Pt_3–Pt_4–X_3; the ground-state mode $X–Pt^{2+}–Pt^{3+}–X–Pt^{3+}–Pt^{2+}–X$ was predicted to be more stable in the order of $X = Cl < Br < I$ [41].

3.7. Vibronic state in the intermediate phase

Toriumi et al. reported on the possible existence of an intermediate phase ($225 < T < 365$ K) in $Pt_2(dta)_4I$ from X-ray single-crystal analysis: A disordered component of the dta ligands was observed for the intermediate phase, in addition to the ordered dta ligands. The four dta planes of the disordered component stand upright almost parallel to the chain axis, while those of the ordered ones are inclined at about 20°. The disordered site occupancy increases with temperature [38].

The standing component of the ligand may imply an elongation of the Pt–Pt distance in the dimer unit. The intermediate phase is a crossover of insulating and metallic states. Possibly, the localized electrons are activated thermally and transferred to neighbor sites as the temperature is increased. If the vibronic coupling is strong in this system, we might imagine that life time of the excited state is not so short. It may be expected that the excited state of mode (2) is miscible with the Mott-Hubbard semiconducting state (3). We imagine that the elongated component is the excited state (2), which is consistent with the observed increase in its occupancy with temperature. Detailed X-ray structural analyses are in progress [39].

4. Conclusions

The MMX-chain system, $Pt_2(dta)_4I$, was found to exhibit metallic conduction above 300 K, which is the first example of a metallic halogen-bridged 1-D transition-metal complex. The metal–insulator transition occurs at 300 K, originating from the Mott transition. The low-temperature charge ordering mode was found to be an alternating charge-polarization state. The highly conductive intermediate phase with a strong electron-lattice interaction is expected to be a unique 1-D spin-charge-lattice coupled system and further investigations are in progress to explain the vibronic state.

Acknowledgements

The authors wish to thank Professor P. Day for his continuous encouragement. We also thank Professors M. Yamashita, K. Toriumi, R. Ikeda, K. Prassides, and

S.A. Borshch for stimulating discussions. We are also indebted to N. Onodera, T. Sonoyama, and M. Yamamoto of JAIST for their help with measurements. Thanks are also due to the Research Center for Molecular Materials, the Institute for Molecular Science, for assistance in obtaining the XPS spectra. This work was partly supported by Grand-in-Aid Scientific Researches no. 09640686 and no. 401 of Priority Areas from the Ministry of Education, Science, Sports and Culture, Japan, and by the Japan Securities Scholarship Foundation.

References

[1] H.J. Keller, in: J.S. Miller (Ed.), Extended Linear Chain Compounds, vol. 1, Plenum, New York, 1982, p. 357.
[2] P. Day, in: H.J. Keller (Ed.), Low-Dimensional Cooperative Phenomena, Plenum, New York, 1974, p. 191.
[3] R.J.H. Clark, in: D.E. Brown (Ed.), Mixed Valence Compounds, Reidel, Dordrecht, 1982, p. 271.
[4] H. Okamoto, T. Mitani, K. Toriumi, M. Yamashita, Mater. Sci. Eng. B13 (1992) L9.
[5] S. Yamada, R. Tsuchida, Bull. Chem. Soc. Jpn. 29 (1956) 894.
[6] Y. Wada, T. Mitani, M. Yamashita, T. Koda, J. Phys. Soc. Jpn. 54 (1985) 3143.
[7] H. Okamoto, T. Mitani, K. Toriumi, M. Yamashita, Phys. Rev. B42 (1990) 10381.
[8] R.J.H. Clark, M. Franks, W. Trumble, Chem. Phys. Lett. 41 (1976) 289.
[9] R.J.H. Clark, M. Kurmoo, Inorg. Chem. 19 (1980) 3522.
[10] H. Tanino, K. Kobayashi, J. Phys. Soc. Jpn. 52 (1983) 1446.
[11] H. Tanino, J. Nakahara, K. Kobayashi, J. Phys. Soc. Jpn. 49 (1980) 695.
[12] M. Tanaka, S. Kurita, T. Kojima, Y. Yamada, Chem. Phys. 96 (1985) 343.
[13] N. Kuroda, M. Sakai, Y. Nishina, M. Tanaka, S. Kurita, Phys. Rev. Lett. 58 (1987) 2122.
[14] N. Matsushita, N. Kojima, T. Ban, I. Tsujikawa, J. Phys. Soc. Jpn. 56 (1987) 3808.
[15] S. Kurita, M. Haruki, K. Miyagawa, J. Phys. Soc. Jpn. 57 (1988) 1789.
[16] R.J. Donohoe, S.A. Ekberg, C.D. Tait, B.I. Swanson, Solid State Commun. 71 (1989) 49.
[17] H. Okamoto, T. Mitani, K. Toriumi, M. Yamashita, Phys. Rev. Lett. 69 (1992) 2248.
[18] Y. Iwasa, E. Funatsu, T. Hasegawa, T. Koda, Appl. Phys. Lett. 59 (1991) 2219.
[19] K. Nasu, J. Phys. Soc. Jpn. 52 (1983) 3865.
[20] K. Nasu, J. Phys. Soc. Jpn. 53 (1983) 302.
[21] K. Toriumi, Y. Wada, T. Mitani, S. Bandow, M. Yamashita, Y. Fujii, J. Am. Chem. Soc. 111 (1989) 2341.
[22] M. Whangbo, M. Foshee, Inorg. Chem. 20 (1981) 113.
[23] G.T. Gammel, A. Saxena, I. Batistic, A.R. Bishop, S.R. Phillpot, Phys. Rev. B45 (1992) 6408.
[24] B.K. Chakraverty, J. Phys. Lett. (Paris) 40 (1979) L99.
[25] C. Bellitto, A. Flamini, L. Gastaldi, L. Scaramuzza, Inorg. Chem. 22 (1983) 444.
[26] C. Bellitto, G. Dessy, V. Fares, Inorg. Chem. 24 (1985) 2815.
[27] H. Kitagawa, N. Onodera, J.-S. Ahn, T. Mitani, K. Toriumi, M. Yamashita, Mol. Cryst. Liq. Cryst. 285 (1996) 311.
[28] H. Kitagawa, N. Onodera, T. Mitani, K. Toriumi, M. Yamashita, Synth. Met. 86 (1997) 193.
[29] H. Kitagawa, M. Yamamoto, N. Onodera, T. Mitani, Synth. Met. 103 (1999) 2151–2152.
[30] H. Kitagawa, N. Onodera, T. Sonoyama, M. Yamamoto, T. Fukawa, T. Mitani, M. Seto, Y. Maeda, J. Am. Chem. Soc. (1999) in press.
[31] H. Okamoto, T. Mitani, K. Toriumi, M. Yamashita, Mater. Sci. Eng. B13 (1992) L9.
[32] J.W. Bray, L.V. Interante, I.S. Jacob, J.C. Bonner, in: J.S. Miller (Ed.), Extended Linear Chain Compounds, vol. 3, Plenum, New York, 1982, p. 353.
[33] L. Alcácer, in: J.-P. Farges (Ed.), Organic Conductors, Marcel Dekker, New York, 1994, p. 269.
[34] G.A. Sawatzky, E. Antovides, J. Phys. (Paris) C4 (1976) 117.

[35] J.C. Scott, Highly conducting quasi-one-dimensional organic crystals, in: E. Conwell (Ed.), Semiconductors and Semimetals, vol. 27, Academic Press, San Diego, 1988, p. 386.
[36] R.J.H. Clark, Infrared Raman Spectrosc. 11 (1984) 95.
[37] M. Yamashita, Y. Wada, K. Toriumi, T. Mitani, Mol. Cryst. Liq. Cryst. 216 (1992) 207.
[38] K. Toriumi et al., to be published.
[39] S. Nakagami, K. Morii, M. Yamamoto, H. Kitagawa, T. Mitani, to be published.
[40] L.G. Butler, M.H. Zietlow, C.-M. Che, W.P. Schaefer, S. Sridhar, P.J. Grunthaner, B.I. Swanson, R.J.H. Clark, H.B. Gray, J. Am. Chem. Soc. 110 (1988) 1155.
[41] S.A. Borshch, K. Prassides, V. Robert, A.O. Solonenko, J. Chem. Phys., 109 (1998) 4562.